PROCEEDINGS OF THE IV INTERNATIONAL CONFERENCE/HIGH TEMPERATURE CAPILLARITY

JOURNAL OF MATERIALS SCIENCE **40** (2005) 2149–2154

Energetics of polycrystals

M. E. GLICKSMAN
Materials Science & Engineering Department, Rensselaer Polytechnic Institute, Troy, New York 12211, USA

The energetics of polycrystalline solids at high temperatures is treated using topological methods. The theory developed represents individual irregular polyhedral grains as a set of symmetrical abstract geometric objects called average $\mathcal{N}$-hedra (ANH's), where $\mathcal{N}$, the topological class, equals the number of contacting neighbor grains in the polycrystal. ANH's satisfy network topological averages in three-dimensions for the dihedral angles and quadrajunction vertex angles, and, most importantly, can act as "proxies" for irregular grains of equivalent topology. The present analysis describes the energetics of grains represented as ANH's as a function of their topological class. This approach provides a quantitative basis for constructing more accurate models of three-dimensional well-annealed polycrystals governed by capillarity. Rigorous mathematical relations, derived elsewhere, for the curvatures, areas, and volumes of ANH's yields quantitative predictions for the excess free energy. Agreement is found between the analytic results and recently published computer simulations.

1. Background and introduction

The energetics and growth kinetics of polycrystals at high temperatures are important topics regarding microstructure evolution in the solid state. The foundation for understanding grain growth in two dimensions was established about 50 years ago by Smith [1], von Neumann [2], and by Mullins [3]. von Neumann proved that a network of two-dimensional grains or bubbles exhibiting uniform mobility, M, and boundary energies, $\gamma_{\rm gb}$, obeys a simple kinetic law:

$$\frac{{\rm d}a}{{\rm d}t} = \frac{\pi\gamma_{\rm gb}M}{3}(n-6), \quad n \geq 2, \tag{1}$$

where a is the area of a grain in two dimensions ($\mathbb{R}^2$) with n sides or vertices. The von Neumann-Mullins relationship, Equation 1, also referred to as the "$n-6$ rule", is the growth law for isotropic two-dimensional polycrystals dominated by capillarity. It provides an excellent approximation for the behavior of grains forming networks in thin films, or, in general, to situations where one spatial dimension of the polycrystal is suppressed relative to the others [4–7]. It is interesting that the "$n-6$" rule was also known empirically to experimentalists [8, 9] before its mathematical basis was established by the distinguished mathematician von Neumann.

The related excess free energy of a 2-d polycrystal (relative to a single crystal of equivalent area), ΔG_2, is given by the sum of all the edge energies over the polygonal grain perimeters, $P_{\rm i}$,

$$\Delta G_2 = \frac{\gamma}{2}\sum_{\rm i} P_{\rm i}, \tag{2}$$

where the edge energy, γ, is considered only as a function of the temperature. The factor of $1/2$ in Equation 2 accounts for the fact that the summation over the 2-d network redundantly counts the grain boundaries twice. Graner *et al.* [10] showed that the total perimeter of a two-dimensional polycrystal may be written in terms of its grain areas, $A_{\rm i}$, by applying the metric relationship that $P_{\rm i} \approx \sqrt{A_{\rm i}}$, and thus Equation 2 becomes

$$\Delta G_2 = \frac{\gamma}{2}\sum_{\rm i} e(n_{\rm i})\sqrt{A_{\rm i}}, \tag{3}$$

where the coefficients of proportionality $e(n_{\rm i}) \equiv P_{\rm i}/\sqrt{A_{\rm i}}$. Graner *et al.* [10] then analyzed the geometrical relationship between the total perimeter and area for *regular* two-dimensional idealized grains consisting of $n_{\rm i}$ identical curved sides meeting pairwise at 120°. Graner *et al.* found that the proportionality coefficients, $e(n)$, appearing in Equation 3 varied weakly with the number of sides, n. Specifically, Graner *et al.* showed that over the entire range of n-values, i.e., $2 \leq n \leq \infty$, the function $e(n)$ varied from a maximum value of $e(2) \approx 3.78$ to a minimum of $e(n \to \infty) \approx 3.71$. Thus, the energy coefficients for 2-d polycrystals changes less than 2% for any value of n. Euler proved that a sufficiently large space-filling polygonal tessellation in $\mathbb{R}^2$ [4] has an average number of sides per cell, $\langle n \rangle$ that approaches 6, and so Equation 3 relates the *total* free energy of a large network of two-dimensional grains to its total grain area

$$\Delta E_2 = \frac{\gamma_{\rm gb}}{2}e(6)\sum_{\rm i}\sqrt{A_{\rm i}}. \tag{4}$$

Later, Vaz and Fortes [11] confirmed that Equation 4 provides an accurate estimate for the excess free energy of two-dimensional foams.

The structure and energetics of three-dimensional polycrystals, however, remains under theoretical study [12–17], computer simulation [18–23] and experiment [24, 25]. This paper reports on extending the free energy analysis of polycrystals to three-dimensions. Polycrystals in three dimensions are modeled as an idealized network consisting of "average $\mathcal{N}$-hedra," which are objects that may be used to estimate the excess free energy of annealed grains in $\mathbb{R}^3$, by direct analogy with Graner *et al*.'s result in $\mathbb{R}^2$.

2. Geometry of interfaces

Consider the coordinate patch for a small portion of a grain boundary in $\mathbb{R}^3$ as is sketched in Fig. 1. The patch mathematically represents a small area on a differentiable surface or interface. The geometry of such smooth surface elements is given by its local shape matrix [26, 27]

$$\kappa_{ij} = \begin{bmatrix} \kappa_1 & 0 \\ 0 & \kappa_2 \end{bmatrix}, \tag{5}$$

where κ_1 and κ_2 are the principal curvatures at the point in question. The principal curvatures, κ_1 and κ_2 are the reciprocals of the two principal (maximum and minimum) radii of curvature, R_1 and R_2, as sketched in Fig. 1.

Two independent scalar invariants may be derived from the matrix, Equation 5. The first represents the mean curvature, H, defined as one-half the trace of the shape matrix, [27],

$$H \equiv \frac{1}{2} Tr \begin{bmatrix} \kappa_1 & 0 \\ 0 & \kappa_2 \end{bmatrix} = \frac{1}{2}(\kappa_1 + \kappa_2), \tag{6}$$

whereas the second represents the Gaussian curvature, K, defined as the determinant of Equation 5,

$$K \equiv Det \begin{bmatrix} \kappa_1 & 0 \\ 0 & \kappa_2 \end{bmatrix} = \kappa_1 \kappa_2. \tag{7}$$

The two curvatures characterize the local geometry of an interface over a sufficiently small and uniform area. Note that H and K have different physical units and represent independent aspects of the local geometry. Specifically, the mean curvature, H, relates changes of area, A, to the volume, V, swept by the surface moving through its surrounding space, $\mathbb{R}^3$. The mean curvature also equals the differential coefficient relating this area and "swept" volume,

$$H = \frac{1}{2} \frac{\delta A}{\delta V}. \tag{8}$$

The Gaussian curvature, by contrast, provides a geometric property that relates to the topological, or intrinsic properties of surfaces. Specifically, the Gaussian curvature, K, equals the change in the "spherical image" projected by a surface, as measured by its subtended solid angle, Ω, with the change in its area, A. Thus, the Gaussian curvature equals the differential coefficient

$$K = \frac{\mathrm{d}\Omega}{\mathrm{d}A}. \tag{9}$$

As such, the total integral of the Gaussian curvature over the surface enclosing any smooth, closed object in $\mathbb{R}^3$ equals 4π steradians. Thus, for any sufficiently *smooth* closed object in $\mathbb{R}^3$, independent of its overall shape, it holds that

$$\iint K \,\mathrm{d}A = 4\pi. \tag{10}$$

Equation 10 provides a convenient starting point for analyzing the properties of grains in a space-filling polycrystal. For the specific case of an equicurved spherical interface, such as a curved grain surface, it also may be shown [28] that H and K are related as

$$K = H^2. \tag{11}$$

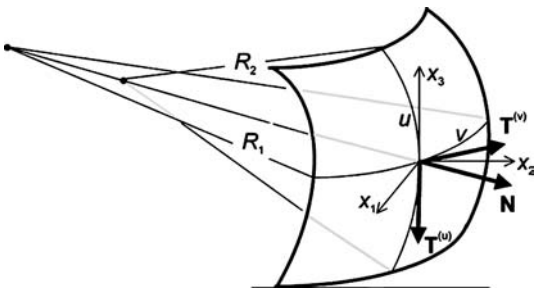

Figure 1 Coordinate patch of a curved interface. The local surface normal, **N** and the pair of tangent vectors $\mathbf{T_u}$ and $\mathbf{T_v}$ define local surface coordinates, (u, v), that specify the principal radii of curvature, R_1 and R_2.

3. Polycrystalline grains

3.1. Irregular polyhedra

Three-dimensional polycrystals, after annealing at high temperature to remove plastic strain, consist of polydisperse space-filling irregular polyhedra. Irregular polyhedral grains consist of a variable number, $\mathcal{N}$, of curved faces. The faces themselves may comprise a variety of shapes from triangular, quadrilateral, pentagonal, hexagonal, etc. As mentioned, the topological rules appropriate to networks in $\mathbb{R}^3$ demand that an individual grain face with p unequal edges ($p = 3, 4, 5, \ldots$) intersects with each of its p neighboring faces on the grain and with one additional face on a neighboring grain to establish a total of $3(\mathcal{N}-2)$ edges, which are the triple-lines of the polycrystal. Thus, any grain in an annealed polycrystal with $\mathcal{N}$ faces ($\mathcal{N} \geq 3$) obeys the rule that its average number of edges per face, $\langle p \rangle$, is given by the topological equation [1]

$$\langle p \rangle = \frac{1}{\mathcal{N}} \sum_{i=1}^{\mathcal{N}} p_i = 6\left(1 - \frac{2}{\mathcal{N}}\right). \tag{12}$$

In addition, annealed irregular grains exhibit trihedral vertices, where the grain's edges intersect three at a time. The total number of trihedral vertices on any irregular grain with $\mathcal{N}$ faces is therefore exactly 2/3 the

Figure 2 A network polyhedron typical of grains found within an annealed three-dimensional polycrystal. Polyhedral grains that fill space are irregular, exhibiting $\mathcal{N}$ "mixed" faces ($\mathcal{N} \geq 4$) each consisting of p edges ($p = 3, 4, 5, 6 \ldots$) of different lengths, intersecting three at a time to form an even number ($2(\mathcal{N}-2)$) of trihedral vertices. The surface properties, such as the mean and Gaussian curvatures, are discontinuous at edges and vertices.

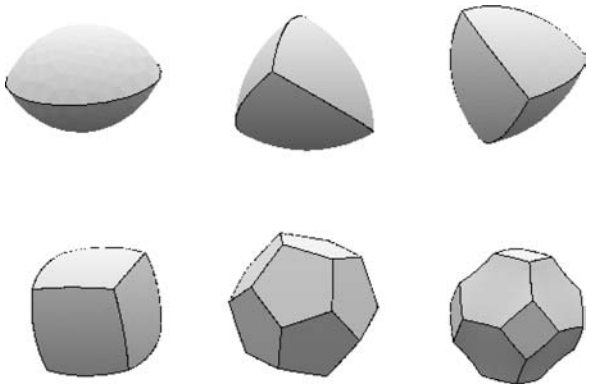

Figure 3 The top row displays constructible ANH's for $\mathcal{N} = 2$, 3, and 4, and the second row (left and middle) displays the remaining two constructible ANH's, $\mathcal{N} = 6$, and 12. Note that the ANH, $\mathcal{N} = 2$ is not useful as a network proxy, insofar as it lacks trihedral vertices, which are required at the quadrajunctions of a 3-d grain network. The last object on the second row is Kelvin's "tetrakaidecahedron"—a space-filling polyhedron consisting of mixed face shapes (squares and hexagons), which therefore fails to qualify as an ANH. The theory used here shows that the five constructible ANH's displayed here have an infinite set of abstract (non-constructible) counterparts for every other integer value of $\mathcal{N}$. The high symmetry of the infinite set of ANH's permits their use as "proxies" for estimating the properties of irregular polyhedra of equivalent topological class.

total number of edges, or $2(\mathcal{N}-2)$. Fig. 2 provides an illustration of a typical (isolated) irregular polyhedral grain showing the relationships among its faces, edges, and vertices. Note, however, that polyhedral grains are not merely smooth bodies: they exhibit singular vertices and edges where the grain boundary curvatures, H and K, appear to be discontinuous.

3.2. Average $\mathcal{N}$-hedra

3.2.1. General

In order to analyze the free energy of three-dimensional polycrystals we now describe the features of a set of geometrical objects termed "average $\mathcal{N}$-hedra" or ANH's. ANH's, although not capable of being constructed or filling space in a 3-d network, nonetheless represent a geometrical generalization, valid for $3 \leq \mathcal{N} \leq \infty$, of the geometrical and topological properties of ordinary, i.e., constructible, space-filling, irregular polyhedra. ANH's, by contrast with irregular polyhedra, have $\mathcal{N}$ identical curved faces that intersect at precisely 120° along $3(\mathcal{N}-2)$ identical edges. The edges meet three at a time at $2(\mathcal{N}-2)$ identical trihedral vertices. All vertices are equidistant from the volume centroid of each ANH. Only four *constructible* examples of ANH's exist that can be used as proxies for irregular network polyhedra [22]: including the cases $\mathcal{N} = 3, 4, 6$, and 12. See examples displayed in Fig. 3.

The "constructibility" of the five ANH's portrayed in Fig. 3 depends on the rather obvious fact that the number of sides per face, which also equals the average number of sides per face, $\bar{p}$, is an integer (1, 2, 3, 4, or 5). Of course, in general, $\bar{p}$ is not an integer, and irregular network polyhedra, such as shown in Fig. 3 often consist of individual faces with a mixed (integer) values of edges (that individually can exceed 6) but overall have a non-integer average number of edges per face, $\bar{p} \leq 6$. Nevertheless, topology requires that the *average* number of sides per face on any polyhedron is *always* equal to

$$\bar{p} = 6 - \frac{12}{\mathcal{N}}, \quad (\mathcal{N} = 3, 4, 5 \ldots \infty) \qquad (13)$$

Unless $\bar{p}$ itself is an integer between 1 and 5, however, the ANH is not "constructible", at least in the ordinary sense of capable of being built or sketched as a physical object in $\mathbb{R}^3$. Thus we find that other ANH's, excepting the five cases for which $\bar{p}$ is an integer, have non-integer $\bar{p}$-values, making them all non-constructible geometrical abstractions. As will be shown, however, ANH's can still usefully serve as accurate "proxies" for irregular polyhedral grains, providing they have the same number of faces, $\mathcal{N}$. Again, grains in real polycrystals consist of space-filling *irregular polyhedra*, exhibiting curved faces that vary in shape (triangles, quadrilaterals, pentagons, hexagons, etc.), and are bounded by sides of varied lengths.

The connection we shall show between irregular grains and their ANH counterparts is that they have identical topological properties, but the latter are easily analyzed regarding their geometric and energetic properties.

4. Space filling in $\mathbb{R}^3$

4.1. Gauss-Bonnet theorem

Polyhedra enclosed by piecewise bounded surfaces obey a fundamental topological sum rule known as the Gauss-Bonnet theorem [26, 27]. The Gauss-Bonnet theorem provides the starting point for the topological description of all objects occupying a volume in $\mathbb{R}^3$. Specifically, if an isolated object is covered at every point on its surface by a unit normal, $\mathbf{n}$, and if a transformation of these normals is applied that maps the normals to the center of a unit sphere, then the infinite set of normals will exactly cover its total surface area of $\Omega_{\text{tot}} = 4\pi$, thereby filling every possible orientation. Moreover, this result is independent of the shape of the body, and provides a basic topological property of all objects existing in $\mathbb{R}^3$.

4.2. Components of the spherical image, Ω_{tot}

The spherical image of any isolated polyhedral body derives from the sum of contributions devolving from its smooth faces, and from all the discontinuities at the polyhedron's curved edges and vertices. One can calculate exactly these contributions for the ANH's because of their ideal symmetry as follows:

1. $\mathcal{N}$ curved faces: $\Omega^{\text{face}} = \iint_{\text{faces}} K\,\mathrm{d}A$.
2. $3(\mathcal{N}-2)$ edges. $\Omega^{\text{edge}} = 3(\mathcal{N}-2)\omega$.
3. $2(\mathcal{N}-2)$ vertices. $\Omega^{\text{vertex}} = 2(\mathcal{N}-2)\Omega_0$.

The total spherical image, Ω_{tot}, of an ANH is the sum of the contributions itemized above, and thus

$$\Omega_{\text{tot}} = \iint_{\text{faces}} K\,\mathrm{d}A + 3(\mathcal{N}-2)\omega + 2(\mathcal{N}-2)\Omega_0 = 4\pi. \tag{14}$$

The contributions to the spherical image from the curved symmetrical edges are proportional to the product of the planar turning angles, ω, between adjacent vertices, and to twice the cosine of the exterior dihedral angle across each edge, the latter of which is just a constant equal to 1 in all cases, because $2\cos(\pi/3) = 1$. The turning angle between vertices, ω, which does vary with $\mathcal{N}$, may be determined by elementary methods from the symmetry properties of the average $\mathcal{N}$-hedra as

$$\omega = \pi + 2\arctan\left(\sin\frac{\alpha}{2}\tan\frac{\pi}{\bar{p}}\right) - 2\arccos\left(-\frac{1}{3}\right), \tag{15}$$

where α is the exterior angle between the face normals located at the geometric center of adjacent faces on the average $\mathcal{N}$-hedron. This angle is the following function of $\mathcal{N}$,

$$\alpha = 4\arctan\sqrt{1 - 2\sec\left(\frac{\pi}{2\,(\mathcal{N}-2)}\right)\cos\frac{\pi\,(2\mathcal{N}-3)}{6\,(\mathcal{N}-2)}} \qquad (\mathcal{N} \geq 4). \tag{16}$$

Polycrystals always have three grains meeting along each triple line. The average interior dihedral angle averaged over the network is therefore $2\pi/3$. An average dihedral angle of $2\pi/3$ is consistent with a quadrajunction, where four grains touch, having meeting angles between edges that are equal on average to the tetrahedral angle, $\arccos(-\frac{1}{3}) \approx 109.47^\circ$. Finally, it may be shown that each equilibrium vertex on any network polyhedron contributes a fixed amount to the spherical image, Ω_0, given by an expression derived by DeHoff [29],

$$\Omega_0 = 2\pi - 3\arccos\left(-\frac{1}{3}\right) = 0.551287\ldots \tag{17}$$

5. Energetics of 3-d polycrystals

The excess free energy of an isotropic polycrystal in three dimensions is given by the sum of the areas of its grain faces,

$$\Delta E_{\text{poly}} = \frac{\gamma_{\text{gb}}}{2}\sum_{\text{i}} A_{\text{i}}(\mathcal{N}). \tag{18}$$

Recently, Cox and Fortes [22] showed by computer simulations that a method similar to that used by Graner *et al*. [10] for determining the free energy of a 2-d isotropic polycrystal (See again **Section 1—Background and Introduction**) also exists for three dimensions. Specifically, Cox and Fortes showed that the analog of Equation 3 in $\mathbb{R}^3$ is

$$\Delta E_{\text{poly}} = \frac{\gamma_{\text{gb}}}{2}\sum_{\text{i}} e_{\text{i}}(\mathcal{N})V_{\text{i}}^{\frac{2}{3}}, \tag{19}$$

where the coefficients $e(\mathcal{N}) = A/V^{2/3}$ are scale-independent metric ratios of the area and volume of each grain. Equation 19 is easily evaluated employing elementary expressions derived elsewhere for the exact areas, volumes, and radii of curvature for the set of ANH's [30, 31]. Indeed, as shown in Fig. 4, $e(\mathcal{N})$ also varies weakly with $\mathcal{N}$, as shown by direct simulation in [22]. Fig. (4) provides a comparison of the analytic results obtained from Equation 19 for ANH's over the range of $\mathcal{N}$-values reported by Cox and Fortes for a few regular polyhedra, using simulations with Brakke's surface evolver [18, 19], and by Cox [23] for many irregular polyhedra. The values for $e(\mathcal{N})$ determined analytically for ANH's agree well with the simulated

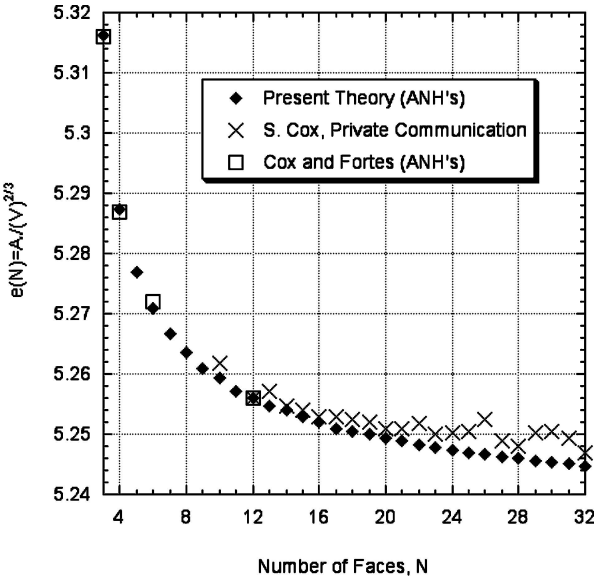

Figure 4 Comparison of computer simulations [22] with the present analysis of the dimensionless surface area, $e(\mathcal{N}) = A(\mathcal{N})/V^{\frac{2}{3}}$. This scale-independent ratio is proportional to the excess free energy of three-dimensional polyhedra. The surface area ratio $e(\mathcal{N})$ varies with $\mathcal{N}$ within a very narrow range of values. The square symbols are data from computer simulations of the four constructible average ANH's ($\mathcal{N} = 3, 4, 6$ and 12). The crosses are more recent data contributed by S. Cox [23] for other irregular constructible polyhedra. Even these data exhibit values no more than $\approx 0.1\%$ larger than those for the corresponding ANH as determined with the present theory.

values, especially for those four cases ($\mathcal{N} = 3, 4, 6,$ and 12), where the constructible polyhedra used in the simulations are ANH's. Where these polyhedra are irregular, they still exhibit scaled areas ($A/V^{\frac{2}{3}}$) that are within about 0.1% of the values for their representative ANH's. This strongly suggests that ANH's can be used to estimate accurately the free energy of an annealed polycrystal.

DeHoff [29] and others [32] showed that the average number of faces per grain in a three-dimensional polycrystal is between 13 and 14 ($\langle\mathcal{N}\rangle \approx 13.4$). Of course such an "average grain" does not exist, because it lacks an integer number of faces. Nonetheless, the value of the average proportionality constant between area and volume, $e(\langle\mathcal{N}\rangle) \approx 5.254$, so the excess free energy of a unit volume of a 3-d polycrystal may be written as the sum over each grain, i,

$$\Delta E_{\text{poly}} \approx 2.63\ \gamma_{\text{gb}} \sum_{i=1}^{n_v} V_{\text{i}}^{\frac{2}{3}}, \tag{20}$$

where n_v is the number of grains per unit volume in the polycrystalline network. The quantity n_v is easily measured in a polycrystal using standard metallographic techniques and applying well-known stereological formulas, [33, 34]. The average grain volume is defined as

$$\langle V\rangle = \frac{1}{n_{\text{v}}}. \tag{21}$$

Using the approximation that $\langle V\rangle^{\frac{2}{3}} \approx \langle V^{\frac{2}{3}}\rangle$, Equation 20 may be rewritten as

$$\Delta E_{\text{poly}} = 2.63\ \gamma_{\text{gb}}\ n_v \langle V^{\frac{2}{3}}\rangle \approx 2.63\ \gamma_{\text{gb}}\ n_v \langle V\rangle^{\frac{2}{3}}. \tag{22}$$

Finally, combining the right-hand side of Equation 22 with Equation 21, yields an estimate for the excess free energy per unit volume of an annealed polycrystal solely in terms of the grain density, n_v,

$$\Delta E_{\text{poly}} = 2.63\ \gamma_{\text{gb}}\ n_v^{\frac{1}{3}}. \tag{23}$$

5.1. Free energy dissipation

If Equation 23 is differentiated with respect to time, one obtains the rate of free energy dissipation for capillarity-mediated grain growth in terms of the rate of grain vanishings, which typically occur as some grains lose faces and $\mathcal{N} \to 4$, and the grain rapidly shrinks to extinction,

$$\frac{\mathrm{d}\Delta E_{\text{poly}}}{\mathrm{d}t} = \beta_1\ \gamma_{\text{gb}}\ n_v^{-\frac{2}{3}} \frac{\mathrm{d}n_v}{\mathrm{d}t}. \tag{24}$$

Here, $\beta_1 \approx 0.88$. Equation 24 suggests that the rate of grain vanishings within a polycrystalline network—a topological process—also sets the rate of loss of excess free energy.

By contrast, if Equation 20 is differentiated directly, one obtains another expression for the rate of free energy dissipation based on grain volume changes *between* topological events, i.e., caused by the declining total amount of grain boundary area induced at elevated temperatures by capillary forces. Thus, we also find that

$$\frac{d\Delta E_{\text{poly}}}{dt} = \beta_2\ \gamma_{\text{gb}} \sum_{i=1}^{n_{\text{v}}} V_{\text{i}}^{-\frac{1}{3}} \frac{dV_{\text{i}}}{dt}, \tag{25}$$

where the coefficient $\beta_2 \approx 1.75$. Clearly, the time-averaged rates of free energy dissipation given in Equations 24 and 25 must be identical, it being inconsequential whether the dissipation is calculated from grain vanishings and the declining grain number density, or from the overall grain volume changes, which comprise a collection of capillary-driven metrical processes leading to either volume increases ($\mathcal{N} \geq 14$) or volume decreases ($\mathcal{N} \leq 13$). This implies that topological events, such as grain vanishings, and capillarity processes, such as grain boundary motions, are eventually coupled over time. This coupling permits the establishment of a self-similar grain size distribution in well-annealed polycrystals. Setting equal the right-hand sides of Equations 24 and 25, and slightly rearranging terms, leads to the final result which is a compatibility relationship between the rates of grain vanishings and the overall time rate of scaled volume changes,

$$\frac{\mathrm{d}}{\mathrm{d}t} n_{\text{v}}^{\frac{1}{3}} = \sum_{i=1}^{n_{\text{v}}} \frac{\mathrm{d}}{\mathrm{d}t} V_{\text{i}}^{\frac{2}{3}}. \tag{26}$$

6. Conclusions

1. Average $\mathcal{N}$-hedra (ANH's) are used to represent the topological properties and geometry of grains in a three-dimensional polycrystal. ANH's although neither constructible nor space-filling, can act as "proxies" for constructible irregular polyhedra that are space filling in $\mathbb{R}^3$.

2. The curvatures (both mean and Gaussian), total face areas, and volumes may be found from exact elementary formulas for all ANH's. These formulas are not provided here, but interested readers may find them at [30, 31].

3. As suggested originally by Cox and Fortes [22] the total energy of an isotropic polycrystal may be expressed through the dimensionless ratio of the grain boundary area to the two-thirds power of the grain volume. This ratio was calculated using the exact geometric expressions given here, and compared to recently published computer simulations in Fig. 4. Good agreement is found between analytic theory and simulations.

4. Using the average number of faces per grain derived by deHoff, namely that $\langle\mathcal{N}\rangle \approx 13.397$, the total free energy of an isotropic polycrystal is found to be $\Delta E_{\text{poly}} \approx 2.63\gamma_{\text{gb}} \sum_{\text{i}} V_{\text{i}}^{\frac{2}{3}}$.

5. The dissipation rate of the excess free energy stored in the grain boundaries may used to determine a compatibility relationship between network topological processes, such as grain vanishing, which account for grain growth, and the overall volumetric rates of change of grains within individual topological classes caused by capillarity.

References

1. C. S. SMITH, "Grain Shapes and other Metallurgical Applications of Topology," Chapter in Metal Interfaces (American Society for Metals, Cleveland, OH, 1952) p. 65.
2. J. VON NEUMANN, in "Metal Interfaces, written discussion" (American Society for Metals, Cleveland, OH, 1952) p. 108.
3. W. W. MULLINS, *J. Appl. Phys.* **27** (1956) 900.
4. V. FRADKOV, M. PALMER, J. NORDBERG, M. E. GLICKSMAN and K. RAJAN, *Physica D* **66** (1993) 50.
5. V. E. FRADKOV, M. PALMER, M. E. GLICKSMAN and K. RAJAN, *Acta Metall. Mater.* **42**(8) (1994) 2719.
6. M. A. PALMER, V. E. FRADKOV, M. E. GLICKSMAN and K. RAJAN, *Scripta Met. et Mat.* **30** (1994) 633.
7. M. A. PALMER, M. E. GLICKSMAN, K. RAJAN, V. FRADKOV and J. NORDBERG, *Metall. Mat. Trans. A* **26A** (1995) 1061.
8. E. B. MATZKE, *Am. J. Botany* **33** (1946) 58.
9. *Idem.*, in "Metal Interfaces, written discussion" (American Society for Metals, Cleveland, OH, 1952) p. 110.
10. F. GRANER, Y. JIANG, E. JANIAUD and C. FLAMENT, *Phys. Rev. E.* **63** (2001) 402.
11. M. F. VAZ, M. A. FORTES and F. GRANER, *Phil. Mag. Lett.* **82** (2002) 575.
12. W. W. MULLINS, *J. Appl. Phys.* **59** (1986) 1341.
13. *Idem.*, *Acta Metall.* **37** (1989) 2979.
14. D. WEAIRE and J. A. GLAZIER, *Phil. Mag. Lett.* **68** (1998) 363.
15. J. A. GLAZIER, *Phys. Rev. Lett.* **70** (1993) 2170.
16. C. MONNEREAU and M. VIGNES-ADLER, *ibid.* **80** (1998) 5228.
17. D. WU, Private Communication, 2003.
18. K. BRAKKE, *Exper. Math.* **1** (1992) 141.
19. *Idem.* (http://geom.umn.edu/software/evolver), (2002).
20. C. MONNEREAU, N. PITTET and D. WEAIRE, *Europhys. Lett.* **52** (2000) 361.
21. S. HILGENFELDT, A. M. KRAYNIK, S. A. KOEHLER and H. A. STONE, *Phys. Rev. Lettr.* **86** (2001) 2685.
22. S. J. COX and M. A. FORTES, *Phil. Mag. Lettr.* **83** (2003) 28.
23. S. J. COX, Private Communication, 2003.
24. C. P. GONATUS, J. S. LEIGH, A. G. YODH, J. A. GLAZIER and B. PRAUSE, *Phys. Rev. Lettr.* **75** (1995) 573.
25. J. A. GLAZIER and B. PRAUSE, in "Foams, Emulsions and Their Applications" edited by P. Zitha *et al*. (MIT-Verlag, Bremen, 2000) p. 120.
26. D. STRUIK, "Lectures on Classical Differential Geometry" (Addison-Wesley, Reading, MA, 1950).
27. M. M. LIPSCHUTZ, "Differential Geometry, Schaums Outline Series" (McGraw-Hill, New York, 1981).
28. D. A. DREW, *SIAM J. Appl. Math.* **50** (1990) 649.
29. R. T. DeHOFF, *Acta Metall. Mater.* **42**(8) (1994) 2633.
30. M. E. GLICKSMAN, *Phil. Mag.* **85** (2005) 3.
31. E. W. WEISSTEIN, "Reuleaux Tetrahedron," *MathWorld*, 2004, http://mathworld.wolfram.com/ReuleauxTetrahedron.html.
32. H. S. M. COXETER, M. S. LONGUET-HIGGINS and J. C. P. MILLER, *Phil. Trans. Roy. Soc. London, Series A* **236** (1954) 401.
33. E. E. UNDERWOOD, "Quantitative Metallography, in Metals Handbook," 9th ed. (American Society for Metals, Metals Park, OH, 1985) p. 123.
34. J. C. RUSS, "The Image Processing Handbook," 2nd ed. (CRC Press, Boca Raton, 1995).

Received 31 March
and accepted 18 July 2004